

1 Draft manuscript for resubmission to *Agricultural and Forest Meteorology*

2 **The peaked response of transpiration rate to vapour pressure deficit in field conditions**
3 **can be explained by the temperature optimum of photosynthesis**

4

5 Remko A. Duursma^a, Craig V.M. Barton^a, Yan-Shih Lin^b, Belinda E. Medlyn^b, Derek
6 Eamus^{c,e}, David T. Tissue^a, David S. Ellsworth^a, Ross E. McMurtrie^d

7

8 ^a Hawkesbury Institute for the Environment, University of Western Sydney, Locked Bag
9 1797, Penrith 2751, NSW, Australia.

10 ^b Department of Biological Sciences, Macquarie University, North Ryde, NSW 2109,
11 Australia

12 ^c School of the Environmental Sciences, University of Technology Sydney, PO Box 123,
13 Broadway, NSW 2007, Australia.

14 ^d School of Biological, Earth and Environmental Sciences, University of New South Wales,
15 Sydney, NSW 2052, Australia.

16 ^e The National Centre for Groundwater Research and Training, University of Technology
17 Sydney, PO Box 123, Broadway, NSW 2007, Australia.

18

19

20

21

22

23 **Abstract**

24 Leaf transpiration rate (E) frequently shows a peaked response to increasing vapour pressure
25 deficit (D). The mechanisms for the decrease in E at high D , known as the ‘apparent feed-
26 forward response’, are strongly debated but explanations to date have exclusively focused on
27 hydraulic processes. However, stomata also respond to signals related to photosynthesis. We
28 investigated whether the apparent feed-forward response of E to D in the field can be
29 explained by the response of photosynthesis to temperature (T), which normally co-varies
30 with D in field conditions. As photosynthesis decreases with increasing T past its optimum, it
31 may drive a decrease in g_s that is additional to the response of g_s to increasing D alone. If this
32 additional decrease is sufficiently steep and coupling between A and g_s occurs, it could cause
33 an overall decrease in E with increasing D . We tested this mechanism using a gas exchange
34 model applied to leaf-scale and whole-tree CO_2 and H_2O fluxes measured on *Eucalyptus*
35 *saligna* growing in whole-tree chambers. A peaked response of E to D was observed at both
36 leaf and whole-tree scales. We found that this peaked response was matched by a gas
37 exchange model only when T effects on photosynthesis were incorporated. Furthermore, at
38 elevated $[\text{CO}_2]$, E peaked at higher D . We hypothesize that could be explained by an increase
39 in the T optimum for A , as frequently observed, however we found no support for a higher T
40 optimum for A in elevated $[\text{CO}_2]$ in this study. We conclude that field-based studies of the
41 relationship between E and D need to consider signals related to changing photosynthesis in
42 addition to purely hydraulic mechanisms.

43 **Key-words:** Stomatal control, temperature response, plant water use, elevated CO_2

44

45 **Introduction**

46 The response of transpiration rate (E) to vapour pressure deficit (D) is well characterized
47 (Monteith 1995), but the mechanisms underlying the response are not yet fully understood.
48 At low D , E increases approximately linearly with increasing D . Subsequently, E saturates
49 with increasing D due to decreasing stomatal conductance (g_s). Frequently, but not always, a
50 third phase in the E - D response is observed, in which E decreases at high D (see reviews by
51 Monteith, 1995; Franks et al., 1997). This third phase of the response of E to D is termed the
52 ‘apparent feed-forward’ response (Farquhar, 1978; Monteith, 1995; Franks et al., 1997), and
53 has caused much debate because it is difficult to explain from simple stomatal mechanics.

54 If the response of stomata to increasing D was the result of feedbacks of transpiration on leaf
55 water status alone, we would expect that E would level off with increasing D , rather than
56 decreasing after reaching some maximum value (Farquhar, 1978). A number of authors have
57 proposed hydraulic mechanisms to explain the apparent feed-forward response. Farquhar
58 (1978) argued that a reduction in E at high D can occur if some leaf water loss occurs through
59 the cuticle, and stomata respond to this water loss. In support of this argument, Eamus et al.
60 (2008) confirmed that manipulations of the leaf epidermis (to increase cuticular conductance)
61 affected stomatal responses to D , and showed that feedback processes were sufficient to
62 explain the three phase behaviour (*sensu* Monteith, 1995).

63 An alternative explanation for the peaked response of E to D is a decrease in plant hydraulic
64 conductance with increasing D (Oren et al., 1999; Macfarlane et al., 2004) possibly as a result
65 of cavitation of xylem due to high evaporative demand at high D , or drying soils. Dewar
66 (2002) used a model of this mechanism to explain the reduction in E at high D , and Buckley
67 (2005) provides additional model support for this hypothesis.

68 In this paper, we put forward a potential additional explanation for the apparent feed-forward
69 response, which is based on the observation that stomata respond not only to leaf water
70 status, but also to signals related to photosynthesis. The exact nature of these signals is not
71 yet understood (Mott et al., 2009; Busch 2013), so they are represented minimally (if at all) in
72 mechanistic models of stomatal conductance (Buckley and Mott 2013). It is well established
73 experimentally that photosynthesis (A) and g_s both respond in parallel to changes in many
74 environmental variables. In many cases, changes in photosynthetic (A) capacity can lead to
75 concomitant changes in g_s (Wong et al. 1979, Messinger et al., 2006). This observation has
76 been observed to hold for a wide range of stress responses including photoinhibition (Wong
77 et al., 1985), ozone and acid mist (Barnes et al., 1990), chilling stress (Martin et al., 1981)
78 high temperature stress (Hamerlynck and Knapp, 1996), salt stress (Seemann and Critchley,
79 1985) and transplanting stress (Guehl et al., 1989), but not for oxygen concentration
80 (Farquhar and Wong 1984), nor does g_s decrease in plants where the Rubisco content has
81 been experimentally reduced (see Busch 2013).

82 Since stomatal conductance responds to changes in photosynthetic capacity, hydraulic
83 responses of E to D may be modulated by photosynthetic effects on g_s if photosynthetic
84 capacity is changing at the same time. In field conditions, rising D is generally accompanied
85 by a rise in air temperature (T), which directly affects photosynthetic capacity. Although
86 there are some experiments that have demonstrated a peaked response of E to D when T is
87 held constant (Eamus et al., 2008; Franks et al., 1997; Grantz, 1990; Thomas and Eamus
88 1999) most reports of the apparent feed-forward phenomenon are from studies where both D
89 and T varied. These include field studies (Macfarlane et al., 2004; Meinzer et al., 1997; Pataki
90 et al., 2000; Whitley et al., 2009), and early laboratory studies (West and Gaff, 1976). Thus,
91 reports of a peaked E response are more common when T co-varies with D , than when T is

92 held constant. This accords with the view held by Franks (1997) that a peaked response of E
93 to D is often difficult to demonstrate in laboratory conditions.

94 If T increases with D , there are consequences for photosynthesis and therefore for E .
95 Experiments have shown that g_s responds strongly to T when D is held constant : it increases
96 with T when T is below the photosynthetic optimum (Fredeen and Sage, 1999; Duursma et
97 al., 2013), but decreases when T is above the photosynthetic optimum (Pons & Welschen,
98 2003). To explain the apparent feed-forward response, we can hypothesize that, as D and T
99 increase, A declines past the photosynthetic temperature optimum, which leads to a decline in
100 g_s that is additional to the direct effect of D on g_s and ultimately contributes to the decrease in
101 E .

102 We tested this hypothesis against whole-tree flux and leaf-level gas exchange data from
103 *Eucalyptus saligna* trees growing in whole-tree chambers. The data demonstrate a strong
104 apparent feed-forward effect, with decreases in measured E at high D . As the weather
105 conditions in the chambers tracked ambient, there was a strong correlation between D and air
106 temperature.

107 We compared these data against leaf gas exchange models based on the well-known Ball-
108 Berry-Leuning model of stomatal conductance (Leuning, 1995):

$$109 \quad g_s = g_0 + g_1 \frac{A}{C_a} \cdot f(D) \quad (1)$$

110 where C_a is the atmospheric CO_2 concentration (we assume that at the leaf surface $[\text{CO}_2]$
111 equals C_a , which is a good approximation in well-mixed conditions) g_1 is a constant
112 parameter, and $f(D)$ represents the effects of D on g_s . In this model, the effects of T on g_s
113 operate through the dependence of A on T (Collatz et al., 1991). This dependence
114 successfully combines the effects of T and D on g_s (Leuning, 1995). Depending on the form

115 chosen for $f(D)$, some versions of this model (e.g. Leuning, 1995) predict a peaked response
116 of E to D when T is constant, but other versions (e.g. Ball et al., 1987; Medlyn et al., 2011)
117 do not.

118 To test our hypothesis that the photosynthetic response to T explains the apparent feed-
119 forward response in these field data, we applied both the Leuning (1995) and Medlyn et al.
120 (2011) versions of this model to the data, firstly assuming that temperature does not affect A ,
121 and then including the temperature dependence of A . By comparing the models without the
122 temperature effect, we are able to determine whether the apparent feedforward effect
123 described in the Leuning (1995) model is sufficient to explain the observed D response on its
124 own. By then including the temperature effect on A in the models, we are able to determine to
125 what extent the temperature effect on A is involved in the observed response to D . We do this
126 for a unique model system where A and E are continuously measured for whole trees in
127 outdoor enclosures.

128

129 **Materials and methods**

130 *Whole-tree fluxes of CO_2 and H_2O*

131 We use whole-tree flux measurements from the Hawkesbury Forest Experiment (HFE) (see
132 Barton et al., 2010, for a detailed description). Twelve 10-m tall whole-tree chambers were
133 established in 2006, and a single Sydney blue gum (*Eucalyptus saligna* Sm.) tree was planted
134 in each chamber in April 2007. Final harvest occurred in March 2009. The experiment was a
135 crossed C_a x drought design with three chambers in each of four treatments. Here, we use
136 only the well-watered chambers. The C_a treatments were ambient (*ca.* 380 ppm; aC_a) and
137 ambient + 240 ppm (eC_a). The chambers were climate-controlled; excellent control of

138 temperature and, to a slightly lesser extent, relative humidity, was achieved (Barton et al.,
139 2010; 2012). Chambers were maintained with T_{air} equal to ambient air temperature outside
140 chambers.

141 Whole-tree fluxes of CO_2 and H_2O were measured for each chamber at 14-minute intervals,
142 along with measurements of air temperature (T_{air}) and vapour pressure deficit (D) inside the
143 chambers. Full details of the measurements are provided in Barton et al. (2010).

144 Photosynthetically active radiation (PAR) was measured outside the chambers. We use all
145 available chamber flux data between 14 April 2008 and 5 March 2009, which consists of a
146 near continuous record apart from a period of *ca.* seven weeks (August – September 2008)
147 when chamber heights were extended (Barton et al., 2012). We averaged the 14-minute
148 readings over hourly intervals. We also averaged the fluxes by C_a treatment for illustration of
149 the patterns, but for analysis we used hourly averages by tree only. We used only the well-
150 watered trees in the experiment ($n=3$ for both C_a treatments), and only data where the
151 photosynthetically active radiation (PAR) was over $600 \mu\text{mol m}^{-2} \text{s}^{-1}$, because we are here
152 interested in behavior at high D , when PAR is near-saturating. All fluxes are expressed on a
153 per unit leaf area basis, using estimates of total tree leaf area based on a combination of
154 complete leaf counting (April 2008), destructive harvest (March 2009), and repeated
155 measurements of height growth and litter fall (see Barton et al., 2012).

156

157 *Leaf gas exchange*

158 To confirm that responses at the leaf scale were similar to those observed for whole-tree
159 fluxes, we analyzed T response curves of leaf gas exchange. These measurements were part
160 of full $A-C_i$ response curves, but here we only use the data when C_a was set to ambient
161 conditions (*ca.* 380 ppm), which was always the first measurement. We used a LI-6400

162 portable photosynthesis system (LI-COR, Inc., Lincoln, NE, USA), with the LED light source
163 set to $1800 \mu\text{mol m}^{-2} \text{s}^{-1}$. Measurements were conducted at three or four leaf temperatures
164 (15, 25, 32 and/or 36 °C, in that order) for all twelve chambers in November 2008 (i.e. before
165 the drought treatment). There was no additional control of D , so that D and T co-varied in a
166 similar way to Fig. 1. Erroneous data for one chamber were discarded.

167

168 *Coupled leaf gas exchange model*

169 We used a standard coupled leaf gas exchange model, using the photosynthesis model of
170 Farquhar, von Caemmerer & Berry (1980), and a new stomatal model (Medlyn et al., 2011)
171 which is very similar to a Ball-Berry type model, but also incorporates the idea that stomata
172 are regulated to minimize the amount of transpiration per unit carbon gain. This model does
173 not predict a feed-forward response of g_s to D if temperature is held constant. The model for
174 g_s is given by:

$$175 \quad g_s = g_0 + 1.6 \left(1 + \frac{g_1}{D^{1-k}} \right) \frac{A}{C_a} \quad (2)$$

176 where g_0 is the residual conductance (g_s when A is zero), g_1 is a parameter related to the
177 marginal water cost of carbon ($\lambda = \partial E / \partial A$), k an empirical parameter (that equals 0.5 when
178 the response of g_s to D is optimal, see Duursma et al., 2013), C_a the atmospheric [CO_2]
179 (ppm), and D the vapour pressure deficit (kPa). In the current study we found a robust way of
180 estimating parameters of Eq. (2) using non-linear regression was to rearrange the equation
181 with A/g_s as the dependent variable. Estimated parameter values obtained using the hourly
182 whole-tree chamber flux data were $g_0 = 0.014 \text{ mol m}^{-2} \text{ s}^{-1}$ (SE 0.0013), $g_1 = 2.44$ (SE 0.058)
183 and $k = 0.66$ (SE 0.019).

184 For comparison, we also used the model of Leuning (1995), given by Eq. (3).

185
$$g_s = g_0 + g_1 \frac{A}{(C_a - \Gamma)(1 + D/D_0)} \quad (3)$$

186 We assume that the CO₂ compensation point (Γ) is zero, to be more comparable to Eq. (2).

187 We used this model because, unlike Eq. (2), it does predict a peaked response of E to D .

188 However, we found that when the model was fit to data, we did not observe a decrease in E

189 with D when $D < 5\text{kPa}$ (see Appendix B). For clarity, we only present the results using Eq.

190 (2).

191 The widely used photosynthesis model of Farquhar et al. (1980) is not described here, see for

192 example Medlyn et al. (2002). We use the temperature sensitivity of the maximum electron

193 transport rate (J_{max}) and the maximum rate of Rubisco activity (V_{cmax}) as parameterized for E .

194 *saligna* with a method equivalent to that of Lin et al. (2013), by measuring $A-C_i$ response

195 curves at various leaf temperatures. The parameters V_{cmax} and J_{max} at a standard leaf

196 temperature of 25 °C were estimated from standard $A-C_i$ curves (D. Ellsworth, unpublished

197 data ; see Ellsworth et al., 2012, for a description of the methods used).

198 Dark respiration (R_d) was estimated using Eq. (4), which was parameterized based on Crous

199 et al. (2011).

200
$$R_d = R_{d0} Q_{10}^{(T-25)/10} \quad (4)$$

201 Where R_{d0} is the basal respiration rate at $T_{\text{air}}=25$ °C. All parameter values are summarized in

202 Table 1. We did not attempt to simulate the difference between T_{leaf} and T_{air} , because we lack

203 estimates of boundary layer conductance inside the chambers. We assume throughout that

204 T_{leaf} is equal to T_{air} , which does not affect the main results, but it does affect the location of

205 the T_{air} optimum of E . If $T_{\text{leaf}} - T_{\text{air}} > 0$, the T_{air} optimum for E is lower by $T_{\text{leaf}} - T_{\text{air}}$, because

206 T_{leaf} drives both photosynthetic capacity and D .

207 We simulated the whole-tree fluxes as if the tree behaves as a single leaf. The only
208 adjustment we made was to reduce V_{cmax} and J_{max} (both set to 35% of their leaf-level
209 estimates), to approximately fit the observed whole-tree flux data. We did not attempt to
210 optimize the fit of the model to the data, as the objective was only to demonstrate the
211 responses of A and E to D and T_{air} . We also used the MAESPA model (Duursma & Medlyn
212 2012) to simulate the whole-tree fluxes based on a more rigorous scaling of leaf-level gas
213 exchange to canopy totals. The MAESPA results are not shown because they were
214 qualitatively the same (and quantitatively similar) as simulations of the single-leaf model.

215 *Data analysis*

216 For the hourly whole-tree flux data, we used generalized additive models with automated
217 smoothness selection (package *mgcv* in R 3.0.1; R Development Core Team, 2012) (Wood,
218 2006) to visualize the trends in A with T and E with D and the differences between C_a
219 treatments, using the C_a -averaged flux data. This method does not assume a prior shape of the
220 functional relationships between the variables. We also fit the generalized additive model by
221 whole-tree chamber, from which the location of the peak was estimated. The locations of the
222 peaks are referred to as T_{opt} (T where A is maximum) and D_{opt} (D where E is maximum). To
223 test whether D_{opt} and T_{opt} differed with C_a treatment, we used a two-sample t -test assuming
224 equal variance (with $n=3$). For the leaf gas exchange data, we fitted a second order
225 polynomial to estimate T_{opt} for E and A , with a linear-mixed effects model (package *nlme* in
226 R). From these fits, we used the delta method as implemented in the *car* package (Fox and
227 Weisberg, 2010) to estimate an approximate 95% confidence interval for D_{opt} and T_{opt} .

228

229 **Results**

230 Using the coupled leaf gas exchange model parameterized for *E. saligna*, we modelled A and
231 E along a range of temperatures (T), while at the same time increasing D using the empirical
232 relationship shown in Fig. 1. As expected, A showed a peaked response to T (Fig. 2A, $T_{\text{opt}} =$
233 27.9 °C), and to D (Fig. 2B, $D_{\text{opt}} = 1.7$ kPa). Because the g_s model we used (Eq. (1)) assumes
234 a strong coupling between g_s and A , E also showed a peaked response to T and D (Fig 2A and
235 2B). The T_{opt} for E was much higher than for A (34.2 °C). Similarly, the D_{opt} was higher for
236 E than A (2.8 kPa). Simulations of g_s demonstrated that very different results were obtained
237 when only D was varied, or when D and T co-varied (Fig. 2C). In the latter case, g_s showed a
238 much more rapid decline at high D and demonstrated the characteristic three-phase response.

239 The whole-tree CO_2 flux expressed on a per unit leaf area basis (A_{tree}) showed a peaked
240 response to air temperature (T_{air}) (Fig. 3), and D (Fig. A1). A_{tree} declined to near zero when
241 T_{air} was *ca.* 45 °C. The leaf gas exchange model used either the measured co-variation in D
242 and T_{air} (based on Fig. 1), or used only T_{air} as a driver (with D constant at 1.5 kPa). Results of
243 the two simulations were similar (Fig. 3C), demonstrating that the T_{air} response of A_{tree} was
244 primarily due to direct T_{air} effects (which affects V_{cmax} , J_{max} , their kinetics, and R_d); the
245 influence of increasing D when applied with increasing T was barely evident (Fig 3c). The
246 coupled leaf gas exchange model showed a peaked response in A , and an increase in T_{opt} with
247 elevated C_a (from 27.1 to 30.0 °C) (Fig. 3C). The flux data did not show a significant increase
248 in T_{opt} , as concluded from the tree-level fluxes (Fig. 5A, $p = 0.129$).

249 The whole-tree fluxes of H_2O , expressed per unit leaf area (E_{tree}), also showed a peaked
250 response to D (Figs. 4A and 4B) and T_{air} (Fig. A2). The leaf gas exchange model was used to
251 predict E_{tree} as a function of either D alone (with T_{air} at 25 °C) or with D and T_{air} co-varying
252 (Fig 4C; based on the empirical relationship in Fig. 1). The simulated responses of E_{tree} to D
253 alone differed between the two simulations: the peaked response in E_{tree} only appeared when
254 T_{air} was taken into account, because it drives A_{tree} when T_{air} exceeds the photosynthetic

255 optimum (Fig. 4C). In the gas exchange model, D_{opt} for E increased with elevated C_a (from
256 2.4 to 2.9 kPa). This result was also observed when we used a different stomatal conductance
257 model, that of Leuning (1995) (Eq. (2)) (Fig. B1). The flux data also showed an increase in
258 D_{opt} with eC_a (Fig. 5B, $p=0.028$), from 2.2 to 2.8 kPa, similar to the gas exchange model.

259 To test whether the response of whole-tree fluxes to D and T_{air} were similar to those at the
260 leaf level, we used the leaf gas exchange data to determine T_{leaf} responses of A and E , while D
261 was co-varying naturally (Fig. 6). The response of E to D was qualitatively similar to the
262 whole-tree flux data and simulations, with E reaching a maximum value at a D of 2.45 kPa
263 for ambient C_a (95% CI : 2.22 – 2.69) or 2.91 kPa for elevated C_a (95% CI : 2.44 – 3.38).
264 Although this shift in optimum D is consistent with our expectation, the difference was not
265 significant ($P > 0.1$) as the curve was broader at the leaf-level than for the canopy.

266 **Discussion**

267 Using whole-tree flux and leaf-level gas exchange data on *Eucalyptus saligna*, we
268 demonstrated a strong decrease in E at high D . We advanced a novel hypothesis for the
269 explanation of the peaked response of E to D , based on the strong correlation between T_{air}
270 and D in field conditions, and the assumption that g_s is linked to photosynthetic rate. We
271 argue that the coupling between g_s and photosynthetic rate was necessary to fully explain the
272 response of E to D in field conditions. This assumption is reasonable based on apparent
273 coupling of A and g_s that is employed in Ball-Berry type stomatal models (Leuning, 1995)
274 and has broad experimental support (Wong and Farquhar, 1979), although the nature of this
275 coupling is still under debate (Busch 2013). When T_{air} increases above the optimum for
276 photosynthesis, the decrease in photosynthesis causes a decrease in g_s . If this decrease in g_s
277 with increasing D is steep enough, E declines. A coupled leaf gas exchange model

278 incorporating the photosynthetic temperature dependence was successful in predicting the
279 response of E to D observed in a whole-tree chamber experiment.

280

281 We stress that our hypothesis to explain the peaked response of E to D requires that D and T
282 are correlated, as is always the case in field conditions, but not always in laboratory
283 experiments. For example, a number of studies have demonstrated this ‘apparent feed-
284 forward’ behaviour when D varied but T was held constant (Grantz, 1990; Bunce, 1997;
285 Eamus et al., 2008). Our hypothesized mechanism likely explains many field observations of
286 the peaked response of E to D , as D and T will be nearly always correlated, and
287 photosynthesis responds strongly to temperature (Berry and Björkman, 1980; Medlyn et al.,
288 2002). A field study in a native *Eucalyptus* woodland (Whitley et al., 2008) showed a peaked
289 response of canopy-scale transpiration (estimated from sap flow) to D , with the optimum in
290 the range 2-3 kPa, consistent with our results (Figs. 2 & 4). Some laboratory experiments also
291 allowed D and T to covary. For example, a study used by the review in Farquhar (1978) to
292 demonstrate feed-forward mechanisms (West and Gaff, 1976) allowed D to co-vary with T .
293 We suggest that in those studies, the effect of T on photosynthesis may explain the peaked
294 response of E to D .

295 Our hypothesized mechanism for the peaked E response does not preclude other mechanisms
296 from operating at the same time. For example, it is possible that hydraulic conductance
297 decreases at high D , which can cause a decrease in E at high D (see Buckley, 2005). In our
298 experiment, we lacked the data to test this specific hypothesis. Other hypothesized
299 mechanisms include feedbacks associated with epidermal water relations (Eamus et al.,
300 2008), and a novel mechanism arising from a model that assumes the guard cell equilibrates
301 with the water vapour inside the leaf (Peak & Mott, 2011; Mott & Peak, 2013). These, and

302 perhaps other mechanisms, may operate alongside a photosynthetically-driven decline in E . It
303 has yet to be demonstrated which mechanisms, including the one we propose, are most
304 important in describing the decline in E at high D .

305 Although we argue that the photosynthetic T optimum causes an optimum in the response of
306 E to D , this should not be taken to mean the optimum occurs at the same T . In fact, E peaks at
307 a higher T than A or g_s (Fig. 1, see also Ku et al., 1977). This can be explained by assuming
308 that, in a well-stirred cuvette, $E = g_s D$. When g_s is exactly proportional to $1/D$, then it is easy
309 to see that E remains constant as D is increasing. Therefore, for E to decrease with increasing
310 D , g_s needs to decrease with a slope that is steeper than $1/D$. As a result, the D at which
311 maximum E occurs has to occur at a higher D than that for maximum A .

312 The coupled leaf gas exchange model demonstrated that an increase in the optimum T for
313 photosynthesis in elevated C_a can result in an increase in the D optimum for E (Figs. 3C &
314 4C), and this increase was confirmed for the whole-tree flux data (Fig. 5B). However, the
315 observed increase in the T optimum for A was not statistically significant for either whole-
316 tree flux data, or leaf gas exchange data ($P > 0.05$ for both), because there was substantial
317 scatter around the location of the optimum. An increase in T_{opt} with eC_a has been observed in
318 leaf-scale measurements of A (e.g. Eamus et al., 1995), including for our study species E .
319 *saligna* (Ghannoum et al., 2010). With increasing T , oxygenation by Rubisco is increasingly
320 favoured over carboxylation, so that the amount of carbon lost through photorespiration
321 increases with T . Because elevated C_a decreases oxygenation by increasing $[\text{CO}_2]$ within the
322 chloroplast, this effect diminishes under elevated C_a . As a result, the C_a stimulation of
323 photosynthesis is larger at higher T . This mechanism is incorporated in the model of Farquhar
324 et al. (1980) (see also Long, 1991; McMurtrie and Wang, 1993). However, it has not been
325 previously suggested that this shift in T_{opt} with eC_a could also contribute to a shift in the T
326 optimum for E . Targeted experiments where D , T and $[\text{CO}_2]$ are carefully controlled, and

327 varied in tandem or alone, will help clarify these relationships to the peaked response of E to
328 D .

329 It is well known that elevated C_a can lead to a decrease in g_s and E (Medlyn et al., 2001). Our
330 whole-tree flux data also demonstrated a decrease in E_{tree} , but only when D was less than ca .
331 2.5 kPa (Fig. 4) (see also Barton et al., 2012). When D was larger, eC_a did not decrease E_{tree} ,
332 and even led to an increase in some cases. This observation was matched by the model, when
333 both T_{air} and D were varied (Fig. 4C). This pattern may be explained by the larger stimulation
334 of photosynthesis at high T , which tends to counteract the stomatal closure arising from the
335 effect of high D . These results show that predictions of the effects of elevated C_a on
336 vegetation water use are highly dependent on the interactions with changes in T_{air} .

337 **Conclusions**

338 A better understanding of the mechanisms of the response of plant water use to atmospheric
339 humidity and temperature would lead to improved model-based projections of climate change
340 effects on vegetation water use and carbon uptake. Here we advance an hypothesis that
341 explains the peaked response of E to increasing D , in a way that could readily be incorporated
342 in models. Evidence for the role of temperature in controlling the response of E to D comes
343 from an experiment on trees growing in elevated C_a , which increased the D optimum for E ,
344 consistent with the expectation that elevated $[\text{CO}_2]$ increases the T optimum for A although
345 we were unable to demonstrate this increase empirically.

346 It is difficult to link the D optimum of E to the T optimum of A across studies, because it
347 requires also that we know how D was related to T , which is seldom reported.

348 Our explanation of the peaked E response provides additional evidence for the link between
349 photosynthetic capacity and stomatal conductance, and helps to expand on the exclusively
350 hydraulic framework so often used to explain stomatal responses to variation in D .

351

352 **Acknowledgments**

353 This research was supported by the NSW government Climate Action Grant (NSW
354 T07/CAG/016), and funding by the Australian Government's Department of Climate Change
355 for the Hawkesbury Forest Experiment. We thank Burhan Amiji and Michael Forster for
356 outstanding technical support. The Hawkesbury Forest Experiment is made possible by a
357 close collaboration with Professor Sune Linder (Swedish University of Agricultural Sciences,
358 Sweden), who generously provided the whole-tree chambers.

359

360

361

362 **Tables**

363 **Table 1.** Parameter values used in the coupled leaf gas exchange model. For all simulations,
 364 photosynthetically active radiation (PAR) was set to $1500 \mu\text{mol m}^{-2} \text{s}^{-1}$. Air (leaf) temperature
 365 was either varied or set to $25 \text{ }^\circ\text{C}$, and vapour pressure deficit either varied or was set to 1.5
 366 kPa. The values for parameters V_{cmax} and J_{max} are at $25 \text{ }^\circ\text{C}$.

Parameter	Value	Units	Source
V_{cmax}	89.5	$\mu\text{mol m}^{-2} \text{s}^{-1}$	D. Ellsworth (unpublished data)
J_{max}	145.4	$\mu\text{mol m}^{-2} \text{s}^{-1}$	“
g_0	0.014	$\text{mol m}^{-2} \text{s}^{-1}$	This study
g_1	2.44		“
k	0.66		“
R_{d0}	0.92	$\mu\text{mol m}^{-2} \text{s}^{-1}$	This study, based on Crous et al., 2011
Q_{10}	1.95		“

367

368

369

370

371

372

373 **Figure captions**

374 **Figure 1.** The dependence of vapour pressure deficit (D) on air temperature (T_{air}) for the
375 chamber flux dataset (data are hourly averages, daylight period only). The thick solid line is
376 the fitted power function ($D = 0.000605 * T_{\text{air}}^{2.39}$). The dashed lines are estimates of D when
377 relative humidity (RH) is constant.

378 **Figure 2. A, B.** Simulated leaf-level transpiration (E) and CO₂ assimilation rate (A) using the
379 coupled leaf gas exchange model. For the simulations, D was allowed to co-vary with T_{leaf}
380 using the empirical relationship shown in Fig. 1. Note that the optimum T_{leaf} for E is higher
381 than the optimum T_{leaf} for photosynthesis. **C.** Simulated stomatal conductance (g_s) as a
382 function of D , either by varying both D and T_{leaf} (solid line, same simulations as in panels A
383 and B), or only D (dashed line, with T_{leaf} set to 25 °C).

384 **Figure 3. A.** Measured hourly whole-tree CO₂ flux rates (A_{tree}) as a function of chamber air
385 temperature (T_{air}), for ambient and elevated C_a treatments. **B.** Smoothed regression (see
386 Methods) of the data, showing estimates of the T_{air} at which A_{tree} is optimum as vertical lines.
387 **C.** Simulations of A_{tree} using the coupled leaf gas exchange model (and reduced V_{cmax} and
388 J_{max} , see Methods). The simulations varied both T_{air} and D (solid line) or D only (dashed
389 line).

390 **Figure 4. A.** Measured hourly whole-tree H₂O flux rates (E_{tree}) as a function of chamber air
391 vapour pressure deficit (D), for ambient and elevated C_a treatments. **B.** Smoothed regression
392 (see Methods) of the data. **C.** Simulation of E_{tree} using the coupled leaf gas exchange model
393 (and a reduced V_{cmax} and J_{max} , see Methods). The simulation varied both T_{air} and D (solid
394 line) or D only (dashed line).

395

396 **Figure 5.** Relationships between E_{tree} and D (panel A), and A_{tree} and T_{air} , shown as smoothed
397 regressions (from a generalized additive model fit) fitted by whole-tree chamber. The filled
398 circles indicate the optimum E_{tree} or A_{tree} , the grey areas are approximate 95% confidence
399 intervals for the mean.

400 **Figure 6.** Leaf-level measurements of CO₂ assimilation (A) and transpiration (E) as a
401 function of T_{air} or D . Individual points are means for a chamber at a particular T_{air} setting of
402 15, 25, 32 and/or 36 °C (usually three T_{air} settings per chamber). Solid lines are second order
403 polynomial fits (the quadratic term was always significant, $P < 0.05$).

404

405 **Appendix A**

406 **Figure A1.** Measured hourly whole-tree CO₂ flux rates (A_{tree}) as a function of vapour
407 pressure deficit (D) inside the chamber, for ambient and elevated C_a treatments. **B.** Smoothed
408 regression (see Methods) of the data **C.** Simulation of A_{tree} using the coupled leaf gas
409 exchange model (and reduced V_{cmax} and J_{max} , see Methods). The simulation varied both T_{air}
410 and D (solid line) or D only (dashed line).

411 **Figure A2.** Measured hourly whole-tree H₂O flux rates (E_{tree}) as a function of chamber air
412 temperature (T_{air}), for ambient and elevated C_a treatments. **B.** Smoothed regression (see
413 Methods) of the data. **C.** Simulation of E_{tree} using the coupled leaf gas exchange model (and
414 reduced V_{cmax} and J_{max} , see Methods). The simulation varied both T_{air} and D (solid line) or D
415 only (dashed line).

416 **Appendix B**

417 **Figure B1.** Comparison of two stomatal conductance models and their predictions of the E
418 vs. D dependence (BBOpti, Medlyn et al. 2011; BBLeuning, Leuning 1995). Although the

419 Leuning (1995) model can predict a decrease in E at high D (Dewar 1995), we never
420 observed a peak in the range of observed D (0 – 5.5 kPa) unless g_0 was set to zero, and D_0 to
421 an arbitrarily low value. In the latter case, the model fit very poorly at low D . Parameters
422 values were, $g_1 = 6.63$, $g_0 = 0.014$, $D_0 = 5.01$.

423

424 **References**

- 425 Ball J.T., Woodrow I.E., Berry J.A., 1987. A model predicting stomatal conductance and its
426 contribution to the control of photosynthesis under different environmental
427 conditions. In: Progress in photosynthesis research (ed J. Biggins), pp. 221-224.
428 Martinus-Nijhoff Publishers, Dordrecht, the Netherlands.
- 429 Barnes J., Eamus D., Brown K., 1990. The influence of ozone, acid mist and soil nutrient
430 status on Norway spruce [*Picea abies* (L.) Karst.]. *New Phytol.* 114, 713-720.
- 431 Barton C.V.M., Duursma R.A., Medlyn B.E., Ellsworth D.S., Eamus D., Tissue D.T., Adams
432 M.A., Conroy J., Crous K.Y., Liberloo M., Löw M., Linder S., McMurtrie R.E.
433 ,2012. Effects of elevated atmospheric [CO₂] on instantaneous transpiration efficiency
434 at leaf and canopy scales in *Eucalyptus saligna*. *Global Change Biol.* 18, 585-595.
- 435 Barton C.V.M., Ellsworth D.S., Medlyn B.E., Duursma R.A., Tissue D.T., Adams M.A.,
436 Eamus D., Conroy J.P., McMurtrie R.E., Parsby J., Linder S., 2010. Whole-tree
437 chambers for elevated atmospheric CO₂ experimentation and tree scale flux
438 measurements in south-eastern Australia: The Hawkesbury Forest Experiment. *Agric.*
439 *For. Meteorol.* 150, 941-951.
- 440 Berry J., Björkman O., 1980. Photosynthetic response and adaptation to temperature in higher
441 plants. *Annual Rev. Plant Physiol.* 31, 491-543.
- 442 Buckley T.N., 2005. The control of stomata by water balance. *New Phytol.* 168, 275-291.
- 443 Buckley, T.N., Mott, K.A., 2013. Modelling stomatal conductance in response to
444 environmental factors. *Plant Cell Environ.* 36, 1691–1699.
- 445 Bunce J.A., 1997. Does transpiration control stomatal responses to water vapour pressure
446 deficit? *Plant Cell Environ.* 20, 131-135.
- 447 Busch, F.A., 2013. Opinion: The red-light response of stomatal movement is sensed by the
448 redox state of the photosynthetic electron transport chain. *Photosynthesis Res.* DOI
449 10.1007/s11120-013-9805-6.
- 450 Collatz G., Ball J., Grivet C., Berry J., 1991. Physiological and environmental regulation of
451 stomatal conductance, photosynthesis and transpiration: a model that includes a
452 laminar boundary layer. *Agric. For. Meteorol.* 54, 107-136.
- 453 Crous K.Y., Zaragoza-Castells J., Löw M., Ellsworth D.S., Tissue D.T., Tjoelker M.G.,
454 Barton C.V.M., Gimeno T.E., Atkin O.K., 2011. Seasonal acclimation of leaf
455 respiration in *Eucalyptus saligna* trees: impacts of elevated atmospheric CO₂ and
456 summer drought. *Global Change Biol.* 17, 1560-1576.
- 457 Dewar, R., 1995. Interpretation of an empirical model for stomatal conductance in terms of
458 guard cell function. *Plant Cell Environ.* 18(4), 365-372.

459 Dewar R., 2002. The Ball-Berry-Leuning and Tardieu-Davies stomatal models: synthesis and
460 extension within a spatially aggregated picture of guard cell function. *Plant Cell*
461 *Environ.* 25, 1383-1398.

462 Doughty C.E., Goulden M.L., 2008. Are tropical forests near a high temperature threshold. *J*
463 *Geophys. Res.* 113, G00B07.

464 Duursma R.A., Medlyn B.E., 2012. MAESPA: a model to study interactions between water
465 limitation, environmental drivers and vegetation function at tree and stand levels, with
466 an example application to [CO₂] × drought interactions. *Geosci. Model Dev.* 5, 919-
467 940.

468 Duursma R.A., Payton P., Bange M.P., Broughton K.J., Smith R.A., Medlyn B.E., Tissue
469 D.T., 2013. Near-optimal response of instantaneous transpiration efficiency to vapour
470 pressure deficit, temperature and [CO₂] in cotton (*Gossypium hirsutum* L.). *Agric.*
471 *For. Meteorol.* 168, 168-176.

472 Eamus D., Duff G.A., Berryman C.A., 1995. Photosynthetic responses to temperature, light
473 flux-density, CO₂ concentration and vapour pressure deficit in *Eucalyptus tetradonta*
474 grown under CO₂ enrichment. *Environ. Pollution.* 90, 41-49.

475 Eamus D., Taylor D.T., Macinnis-Ng C.M.O., Shanahan S., De Silva L., 2008. Comparing
476 model predictions and experimental data for the response of stomatal conductance and
477 guard cell turgor to manipulations of cuticular conductance, leaf-to-air vapour
478 pressure difference and temperature: feedback mechanisms are able to account for all
479 observations. *Plant Cell Environ.* 31, 269-277.

480 Ellsworth D.S., Thomas R., Crous K.Y., Palmroth S., Ward E., Maier C., DeLucia E., Oren
481 R., 2012. Elevated CO₂ affects photosynthetic responses in canopy pine and
482 subcanopy deciduous trees over 10 years: a synthesis from Duke FACE. *Global*
483 *Change Biol.* 18, 223-242.

484 Farquhar G., 1978. Feedforward responses of stomata to humidity. *Fun. Plant Biol.* 5, 787-
485 800.

486 Farquhar G.D., Caemmerer S., Berry J.A., 1980. A biochemical model of photosynthetic CO₂
487 assimilation in leaves of C3 species. *Planta*, 149, 78-90.

488 Fox, J., Weisberg, S., 2010. An R companion to applied regression, 2nd ed. Sage
489 Publications, Inc. 472p.

490 Franks P.J., Cowan I.R., Farquhar G.D., 1997. The apparent feedforward response of stomata
491 to air vapour pressure deficit: information revealed by different experimental
492 procedures with two rainforest trees. *Plant Cell Environ.*, 20, 142-145.

493 Fredeen, A.L., Sage, R.F., 1999. Temperature and humidity effects on branchlet gas-
494 exchange in white spruce: an explanation for the increase in transpiration with
495 branchlet temperature. *Trees* 14, 161-168.

496 Ghannoum, O., N.G. Phillips, M.A. Sears, B.A. Logan, J.D. Lewis, J.P. Conroy, D.T. Tissue,
497 2010. Photosynthetic responses of two eucalypts to industrial-age changes in
498 atmospheric [CO₂] and temperature. *Plant, Cell Environ.* 33(10): 1671-1681.

499 Grantz D.A., 1990. Plant response to atmospheric humidity. *Plant Cell Environ.*, 13, 667-679.

500 Guehl J., Aussenac G., Kaushal P., 1989. The effects of transplanting stress on
501 photosynthesis, stomatal conductance and leaf water potential in *Cedrus atlantica*
502 Manetti seedlings: role of root regeneration. *Ann. Sci. For.* 46S, 464-468.

503 Hamerlynck E., Knapp A.K., 1996. Photosynthetic and stomatal responses to high
504 temperature and light in two oaks at the western limit of their range. *Tree Physiol.* 16,
505 557-565.

506 Katul G.G., Palmroth S., Oren R., 2009. Leaf stomatal responses to vapour pressure deficit
507 under current and CO₂-enriched atmosphere explained by the economics of gas
508 exchange. *Plant Cell Environ.* 32, 968-979.

509 Ku S.B., Edwards G.E., Tanner C.B., 1977. Effects of light, carbon dioxide, and temperature
510 on photosynthesis, oxygen inhibition of photosynthesis, and transpiration in *Solanum*
511 *tuberosum*. Plant Physiol. 59, 868-872.

512 Leuning R., 1995. A critical-appraisal of a combined stomatal-photosynthesis model for C-3
513 plants. Plant Cell Environ. 18, 339-355.

514 Lin, Y.-S., Medlyn, B.E., De Kauwe, M.G. and Ellsworth, D.S., 2013. Biochemical
515 photosynthetic responses to temperature: how do interspecific differences compare
516 with seasonal shifts? Tree Physiology. doi: 10.1093/treephys/tpt047

517 Long S., 1991. Modification of the response of photosynthetic productivity to rising
518 temperature by atmospheric CO₂ concentrations: Has its importance been
519 underestimated? Plant Cell Environ. 14, 729-739.

520 Lösch R., 1977. Responses of stomata to environmental factors—experiments with isolated
521 epidermal strips of *Polypodium vulgare*. I. Temperature and humidity. Oecologia. 29,
522 85-97.

523 Macfarlane C., White D.A., Adams M.A., 2004. The apparent feed-forward response to
524 vapour pressure deficit of stomata in droughted, field-grown *Eucalyptus globulus*
525 Labill. Plant Cell Environ. 27, 1268-1280.

526 Martin B., Ort D.R., Boyer J.S., 1981. Impairment of photosynthesis by chilling-temperatures
527 in tomato. Plant Physiol. 68, 329-334.

528 McMurtrie R., Wang Y., 1993. Mathematical models of the photosynthetic response of tree
529 stands to rising CO₂ concentrations and temperatures. Plant Cell Environ. 16, 1-13.

530 Medlyn B.E., Dreyer E., Ellsworth D., Forstreuter M., Harley P.C., Kirschbaum M.U.F., Le
531 Roux X., Montpied P., Strassmeyer J., Walcroft A., Wang K., Loustau D., 2002.
532 Temperature response of parameters of a biochemically based model of
533 photosynthesis. II. A review of experimental data. Plant Cell Environ. 25, 1167-1179.

534 Medlyn B.E., Duursma R.A., Eamus D., Ellsworth D.S., Prentice I.C., Barton C.V.M., Crous
535 K.Y., De Angelis P., Freeman M., Wingate L., 2011. Reconciling the optimal and
536 empirical approaches to modelling stomatal conductance. Global Change Biol. 17,
537 2134-2144.

538 Meinzer F.C., Hinckley T.M., Ceulemans R., 1997. Apparent responses of stomata to
539 transpiration and humidity in a hybrid poplar canopy. Plant Cell Environ. 20, 1301-
540 1308.

541 Messinger, S.M., Buckley, T.N., Mott, K.A., 2006. Evidence for Involvement of
542 Photosynthetic Processes in the Stomatal Response to CO₂. Plant Physiol. 140, 771–
543 778.

544 Monteith J.L., 1995. A reinterpretation of stomatal responses to humidity. Plant Cell Environ.
545 18, 357-364.

546 Mott, K.A., 2009. Opinion: Stomatal responses to light and CO₂ depend on the mesophyll.
547 Plant, Cell Environ., 32(11): 1479-1486.

548 Mott K.A., Peak D., 2013. Testing a vapour-phase model of stomatal responses to humidity.
549 Plant Cell Environ. 36(5), 936-944.

550 Oren, R., Sperry, J.S., Katul, G.G., Pataki, D.E., Ewers, B.E., Phillips, N., Schäfer, K.V.R.,
551 1999. Survey and synthesis of intra- and interspecific variation in stomatal sensitivity
552 to vapour pressure deficit. Plant Cell Environ. 22, 1515–1526.

553 Pataki D.E., Oren R., Smith W.K., 2000. Sap flux of co-occurring species in a western
554 subalpine forest during seasonal soil drought. Ecology. 81, 2557-2566.

555 Peak, D., Mott, K.A., 2011. A new, vapour-phase mechanism for stomatal responses to
556 humidity and temperature. Plant Cell Environ. 34, 162–178.

557 Pieruschka R., Huber G., Berry J.A., 2010. Control of transpiration by radiation. PNAS. 107,
558 13372-13377.

559 Pons, T.L., Welschen, R.A.M., 2003. Midday depression of net photosynthesis in the tropical
560 rainforest tree *Eperua grandiflora*: contributions of stomatal and internal
561 conductances, respiration and Rubisco functioning. *Tree Physiol.* 23, 937–947.

562 R Core Team, 2013. R: A language and environment for statistical computing. R Foundation
563 for Statistical Computing, Vienna, Austria. URL <http://www.R-project.org/>.

564 Rodriguez J.L., Davies W.J., 1982. The effects of temperature and ABA on stomata of *Zea*
565 *mays* L. *J Exp. Bot.* 33, 977-987.

566 Sage R.F., Sharkey T.D., 1987. The effect of temperature on the occurrence of O₂ and CO₂
567 insensitive photosynthesis in field grown plants. *Plant Physiol.* 84, 658-664.

568 Seemann J.R., Critchley C., 1985. Effects of salt stress on the growth, ion content, stomatal
569 behaviour and photosynthetic capacity of a salt-sensitive species, *Phaseolus vulgaris*
570 L. *Planta.* 164, 151-162.

571 Thomas D., Eamus D., 1999. The influence of predawn leaf water potential on stomatal
572 responses to atmospheric water content at constant C_i and on stem hydraulic
573 conductance and foliar ABA concentrations. *J Exp. Bot.* 50, 243-251.

574 West D., Gaff D., 1976. The effect of leaf water potential, leaf temperature and light intensity
575 on leaf diffusion resistance and the transpiration of leaves of *Malus sylvestris*.
576 *Physiol. Plant.* 38, 98-104.

577 Whitley R., Medlyn B., Zeppel M., Macinnis-Ng C., Eamus D., 2009. Comparing the
578 Penman–Monteith equation and a modified Jarvis–Stewart model with an artificial
579 neural network to estimate stand-scale transpiration and canopy conductance. *J.*
580 *Hydrol.* 373, 256-266.

581 Whitley R., Zeppel M., Armstrong N., Macinnis-Ng C., Yunusa I., Eamus D., 2008. A
582 modified Jarvis-Stewart model for predicting stand-scale transpiration of an
583 Australian native forest. *Plant and Soil.* 305, 35-47.

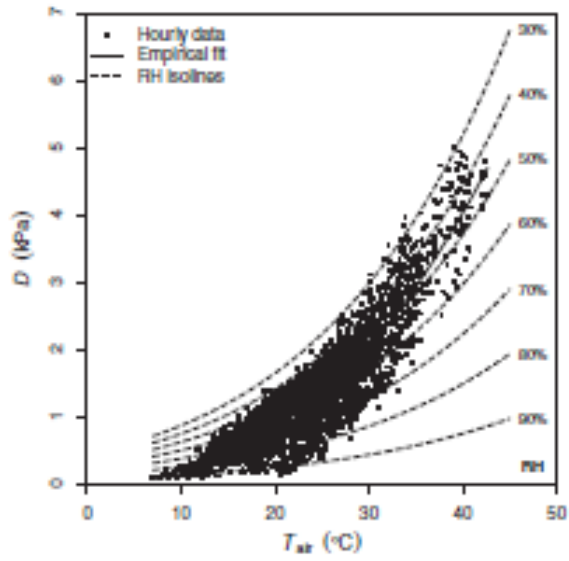
584 Winter K., Aranda J., Garcia M., Virgio A., Paton S.R., 2001. Effect of elevated CO₂ and soil
585 fertilization on whole-plant growth and water use in seedlings of a tropical pioneer
586 tree, *Ficus insipida*. *Flora.* 196, 458-464.

587 Wong S., Cowan I., Farquhar G., 1979. Stomatal conductance correlates with photosynthetic
588 capacity. *Nature*, 282, 424-426.

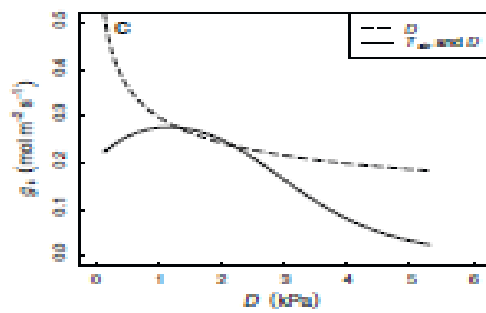
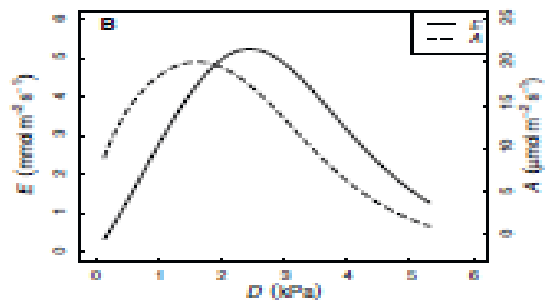
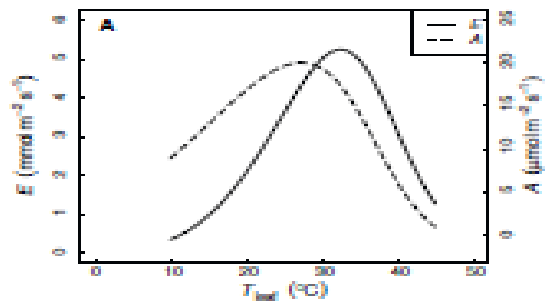
589 Wong S.C., Cowan I.R., Farquhar G.D., 1985. Leaf conductance in relation to rate of CO₂
590 assimilation: III. Influences of water stress and photoinhibition. *Plant Physiol.* 78,
591 830.

592 Wood S.N., 2006. Generalized additive models : an introduction with R. Chapman &
593 Hall/CRC.

594
595
596
597
598
599
600
601
602
603
604
605
606
607
608

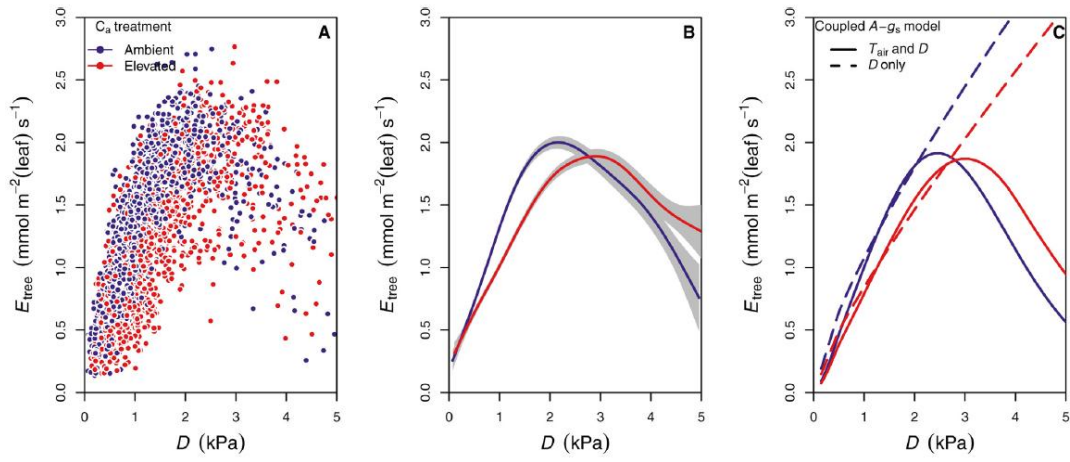


609
 610
 611
 612
 613
 614
 615

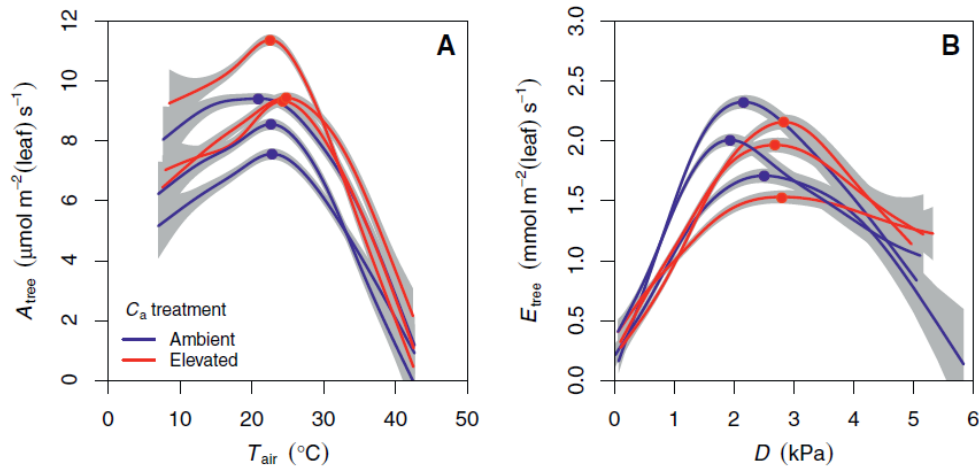


616
 617
 618

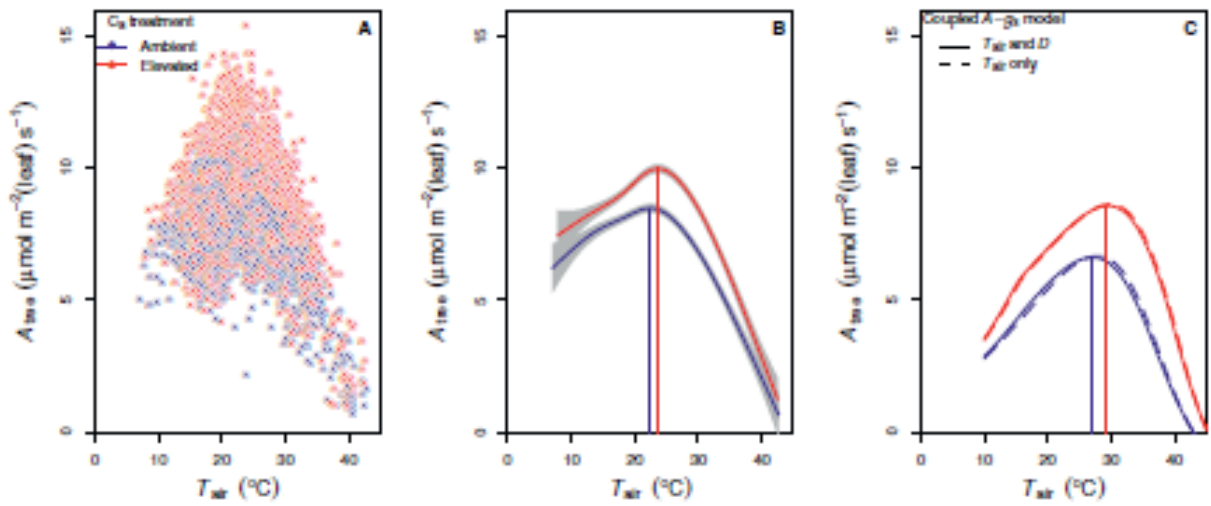
619
620



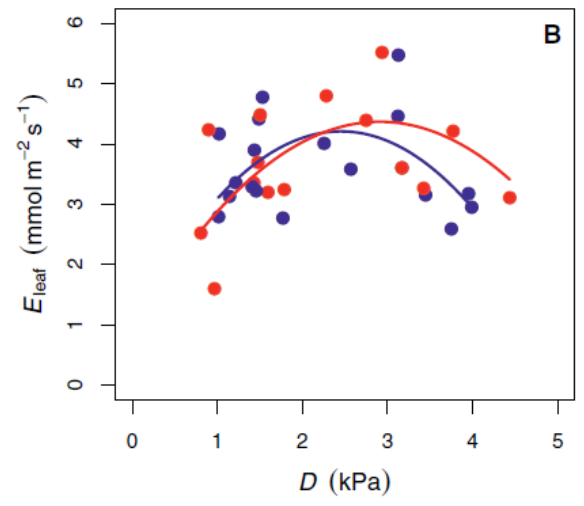
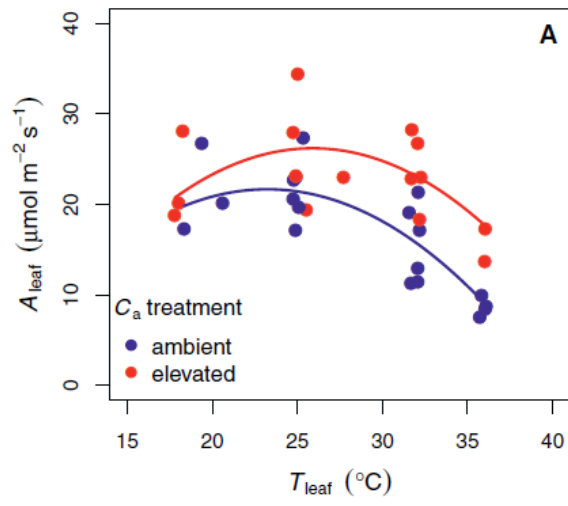
621
622
623
624
625



626
627
628
629
630



631



632